Fabrication of Ideally Ordered Nanoporous Alumina Films and Integrated Alumina Nanotubule Arrays by High-Field Anodization**

By *Song-Zhu Chu*,* *Kenji Wada*, *Satoru Inoue*, *Masafumi Isogai*, and *Atsuo Yasumori*

Self-organized porous alumina nanostructures fabricated by the anodization of aluminum have attracted considerable attention in both scientific and commercial fields as an indispensable part of nanotechnology. This has been fuelled by their versatile applications in fields of electronics or optoelectronics,[1] magnetics,[2,3] energy storage,[4] photocatalysis,[5] photonics,[6] and biosensors.[7] To facilitate various practical applications and nanodevices, fabricating highly ordered porous anodic alumina films with low cost and by a simple process on a large scale is an essential and urgent task and has yet not been solved.

Porous anodic alumina (PAA) films with parallel nanopores are known as having a honeycomb-like structure that has short-distance ordering (in several tens to hundreds of nanometers) but long-distance disordering for pore arrangement.[8] To achieve a highly ordered pore arrangement over a large area, many studies have so far elaborated a variety of pretreatments or pretexturing techniques.[9–15] For instance, Masuda and Fukuda[9] first proposed a two-step anodization process, in which the dents on aluminum formed in the first anodization step (several days) worked as the initial sites of pore growth in the second anodization step, thus improving the overall pore arrangement to some extent. To achieve highly ordered PAA films, Masuda and co-workers also invented a pretexturing process,[10,11] i.e., using a textured SiC molder to produce ordered patterns on aluminum by a mechanical indentation prior to anodization. The shallow concaves on aluminum induced the pore initiation during anodization and led to an ideally ordered pore arrangement within the stamped areas (e.g., 4 mm × 4 mm). Recently, some modified pretexturing methods, such as pre-patterning on aluminum by optical diffraction grating,[12] atomic force microscope scanning probe,[13] focused-ion-beam,[14] and polystyrene beads,[15] have been also attempted, to perform direct or mold-less patterning on aluminum exclusive of the expensive SiC master fabrication. To facilitate pretexturing, aluminum samples were usually annealed in nitrogen or argon at 400–500 °C to remove mechanical stress and to recrystallize the aluminum. They were then electro-polished in mixed acid solutions (e.g., a mixture of $HClO_4$ and C_2H_5OH) to smooth the surface for precise and uniform imprints. However, all of the pretexturing processes mentioned above, i.e., controlling the initial sites of pore growth, are utilizing external methods or extrinsic factors to achieve ordered PAA films. The decisive method or the intrinsic factor for pore ordering, however, is actually the anodizing process itself, i.e., the optimally combined anodizing conditions such as solution, temperature, and potential or current density. Therefore, raising the self-organizing ability of porous alumina films through an anodizing process, exclusive of any external assistance, is the radical solution for lowering production cost and exploring new applicable fields, which are significant in both fundamental science and commercial applications.

Anodization for self-organized PAA films is usually performed in various acid solutions, such as sulfuric, oxalic, and phosphoric acids.[10,16–20] Generally, highly ordered PAA films assisted by pretexturing were mostly formed in oxalic solutions at potentials of 40–80 V.[10,20] In contrast, the pore arrangement of PAA films formed in sulfuric solutions at low potentials (< 25 V) was relatively irregular.[16] Stable anodization in sulfuric solutions was usually difficult to maintain over 27 V, because of the occurrence of breakdown or 'burning' of alumina films due to corrosive acid attack under a high electric field. Recently, Shingubara et al. successfully formed PAA films at 36 V in a dilute sulfuric acid solution,[19] while the regularity of the pore arrangement is similar to that formed at 25–27 V.[16,20] Since sulfuric acid electrolytes are the most commonly used in industry due to their low cost and ease of handling for circumstance, finding appropriate anodizing conditions for the fabrication of highly ordered PAA films in sulfuric acid solutions is significant from the viewpoint of practical applications.

In the present communication, we report a simple and low-cost approach to fabricate large-area highly ordered nanoporous alumina films in sulfuric acid solutions through a single-step high-field anodization, without the assistance of any additional process including the routine pretreatments of annealing and electropolishing. The central idea of our approach is to raise anodizing potentials by adjusting the solution states. In preliminary experiments, we found that the critical high anodizing potential, i.e., the break-down or burning potential of PAA films in the electrolyte system adopted, increased with the ageing of solutions after a long period of anodization, experimentally 10–20 ampere hours per liter. Correspondingly, the applicable current density for stable an-

[*] Dr. S. Z. Chu,[+] Dr. K. Wada, Dr. S. Inoue
Advanced Materials Laboratory
National Institute for Materials Science (NIMS)
Namiki-1, Tsukuba, Ibaraki, 305-0044 (Japan)
E-mail: chusongz@criepi.denken.or.jp
M. Isogai, Prof. A. Yasumori
Department of Materials Science and Technology
Graduate School of Industrial Science and Technology
Tokyo University of Science
2641, Yamazaki, Noda, Chiba 278-8510 (Japan)
[+] Present address: Materials Science Research Laboratory, Central Research Institute of Electric Power Industry (CRIEPI), Nagasaka 2-6-1, Yokosuka, Knagawa, 240-0196, Japan.

[**] This work is part of the Japan Millennium Project of "Exploration and Creation of a Catalyst for Removing Harmful Chemical Substances".

 DOI: 10.1002/adma.200500401

ADVANCED MATERIALS

odization also rose significantly, thus leading to a high-speed film-growth. As a result, we successfully achieved uniform PAA films in sulfuric acid solutions under a high electric field of 40–70 V and 1600–2000 A m^{-2}, which is much higher than ordinary anodization (< 27 V, < 200 A m^{-2}).

Figure 1 exhibits representative PAA films formed under different anodizing conditions. The self-organization of the films apparently proceeds as the anodizing potentials increase. A highly ordered pore arrangement with hexagonal texture is

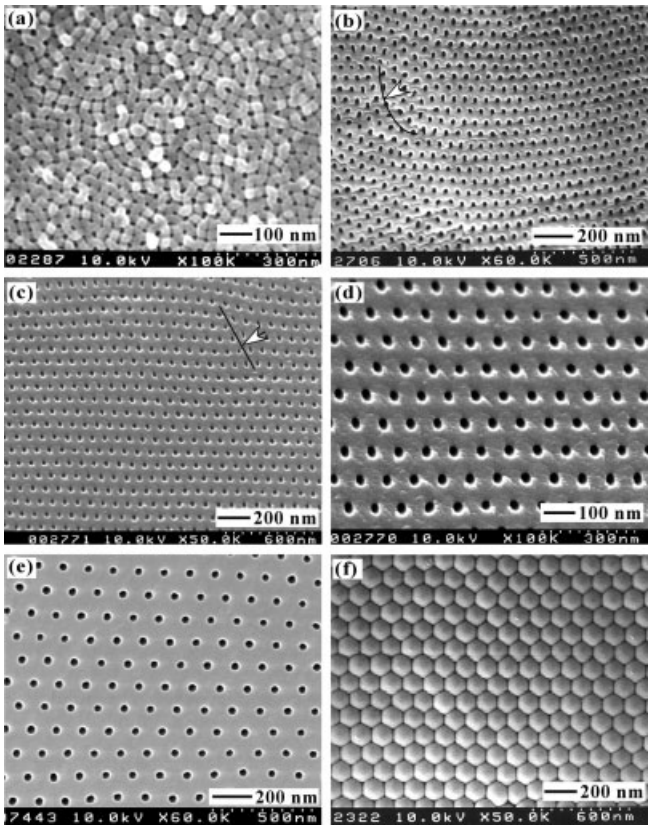

Figure 1. Field-emission scanning electron microscope (FESEM) images of highly ordered nanoporous anodic alumina films formed in a sulfuric acid solution at a) 15 V, 150 A m^{-2}, 5 °C; b) 25 V, 150 A m^{-2}, 0.1 °C; c,d) 40 V, 1600 A m^{-2}, 0.1 °C; e,f) 70 V, 2000 A m^{-2}, 0.1 °C. a–e) Transverse fracture sectional images. f) Bottom view from the barrier layer side.

achieved within domains that are separated by grain boundaries from neighboring domains with different orientation of pore lattice. With increasing electric field, i.e., anodizing potential and current density, the extent of the order of the pore arrangement inside the domains and throughout the overall specimens is significantly improved, and the size of the ordered domains is also increased correspondingly. The most highly ordered PAA films (ϕ 50 nm, ≈ 130 nm interval) with a perfect honeycombed hexagonal array are achieved under 70 V and 2000 A m^{-2} (Figure 1f), which is the highest electric field attained for the electrolyte system we used. This result is consistent with the hypothesis that was recently proposed by Ono et al.,[20,21] in which a high current density or high electric-field strength is a key controlling factor for the self-ordering of PAA films. Moreover, it should be noticed that the disordering of a pore lattice at the interfaces of domains (arrows in Figs. 1b,c) abates or disappears gradually with increasing electric field. This indicates that the influence of gain or crystal size of the aluminum materials on the pore arrangement tends to be eliminated under high-field anodization, thus leading to highly ordered PAA films over large areas. In addition, it is also found that the appearance of the PAA films formed under high fields (40–70 V) exhibited a dark-yellow color with high hardness and stress, in contrast to the colorless, transparent PAA films formed under potentials lower than 25 V. According to the results of energy-dispersive X-ray (EDX) analysis (not shown), a small amount of sulfur (3–5 at.-%), due to sulfuric anion incorporation, was detected in the PAA films, irrespective of the anodizing potentials. This indicates that the variation in appearance of the high-field PAA films is not ascribed to the chemical composition but to some physical properties, such as density of anodic alumina, porosity of films, etc.

The effects of electric field (simplified as anodizing potentials, E_a) on the self-organization of PAA films are summarized in Figure 2. The average pore interval (Δ_{int}) and average pore size (ϕ) are linearly proportional to the anodizing potential (Fig. 2a, the left axis), in accordance with the theory established by Wood et al.[8] ($\Delta_{int} = \Delta_{cell} = 2\delta_{barrier} + \phi$; where Δ_{cell} is the cell size, $\delta_{barrier}$ is the thickness of the barrier layer, and $\delta_{barrier} \propto E_a$). Notably, the size of the self-ordering regime of the PAA films (Fig. 2a, the right axis) exhibits an abrupt increment as the anodizing potential changes from a low-field region (lower than 20 V) to 25 V. This value (25 V) is actually the critical high potential of stable anodization for the 'fresh' sulfuric acid solution we used. With an increase in the electric field, by adjusting the solution ageing state and temperature, the size of the self-ordering regime increases linearly with anodizing potential, giving the largest ordering regime of ≈ 6 micrometers at 70 V. Considering the fact that we used as-received aluminum without pretreatment and pre-patterning, and that we performed a one-step anodization in a short period (20 min), the self-ordering effect at high electric fields is quite promising. Because the defects or the distortion of the pore lattice in the PAA films usually appear at the boundaries between domains or grains, it is predictable that the self-ordering may be further improved through conventional annealing and electropolishing to aluminum. This is due to the known stress-releasing and/or grain-merging effects (the former) and the surface roughness decreasing (the latter). Moreover, since the self-organization of PAA films is proportional to anodizing time,[16] the ordered regimes can be further improved after a long period of anodization.

Figure 2b gives the ratios of Δ_{int} to E_a and the porosities of the films formed at different potentials. Interestingly, the Δ_{int}/E_a ratio is not a constant but demonstrates a reverse relation to anodizing potential (Fig. 2b, the left axis), which can be ascribed to the interacting repulsive force between the alumina

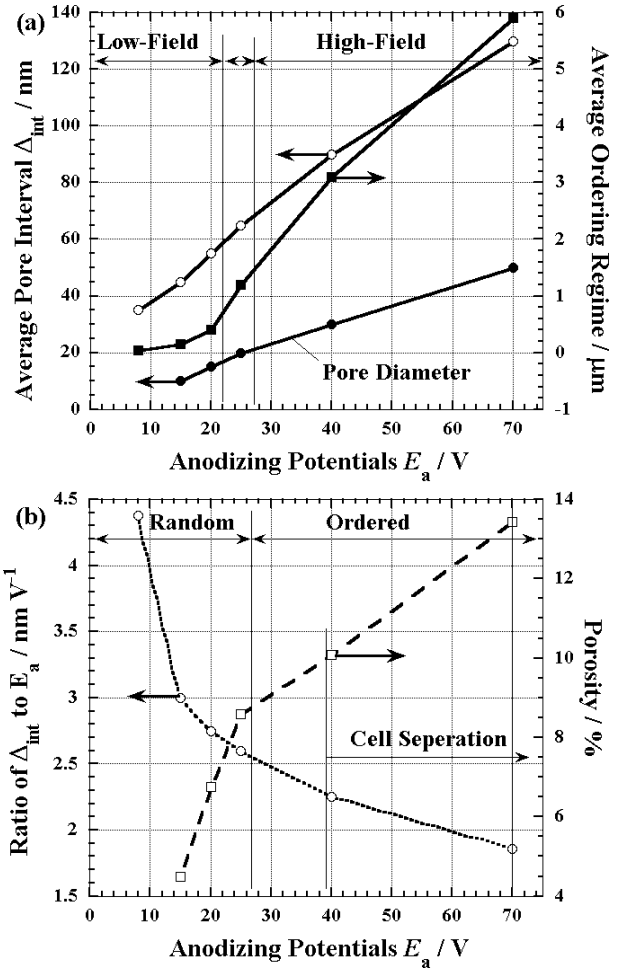

Figure 2. Effects of anodizing potential on the self-ordering of porous anodic alumina films.

cells that is associated with the expansion during oxide formation at the aluminum/oxide interface.[8,22] The expansion force increases with electric field, due to the high-speed formation of alumina at the semi-spherical pore tips under high potential and high current density. It is the strong repulsive or expansion force under high field (40–70 V) that limited the transverse growth of alumina cells and forced them to adopt the mostly closed geometric space arrangement, i.e., the ideally hexagonal arrays, thus producing the highly ordered PAA films over large areas. Moreover, since the pore arrangement within the domains is hexagonal, the porosity of the porous alumina nanostructures can be calculated by:

$$P = \frac{2\pi}{\sqrt{3}}\left(\frac{r}{\Delta_{int}}\right)^2 \quad (1)$$

where r is the pore radius, and Δ_{int} is the pore interval or cell size.

The porosity of the films (Fig. 2b, right axis) increases as the anodizing potential increases, which can be ascribed to the high current density and strong chemical dissolution enhanced by the electric field. In particular, the ordered PAA films formed at high fields possess a porosity of 10–13.5 %. This is consistent with a hypothesis proposed by Nielsch et al.,[23] in which a 10 % porosity theory was proposed as a requisite condition for the self-ordering of a pore arrangement based on the volume expansion from alumina to porous alumina.

Another interesting phenomenon accompanied by high-field anodization is the variation of the junction strength of the alumina cells in the PAA films. Figure 3 shows the different fractured modes in the vertical direction of PAA films formed at 25 and 40 V. For the films formed at potentials lower than 25 V (Fig. 3a, low field), the cleavage planes are

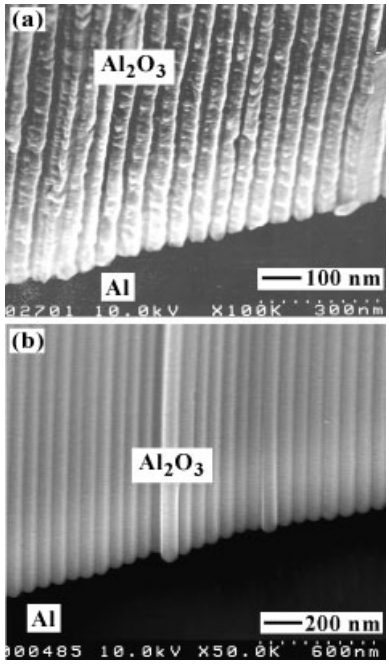

Figure 3. FESEM images of vertical fracture sections of porous anodic alumina films formed at a) 25 V and b) 40 V. Before imaging, the specimens were immersed in a 5 % H_3PO_4 solution for ≈ 1 min to clearly show the pore channels.

mostly across the central lines of the pore arrays, which are mechanically weak. For films obtained at potentials over 40 V (Fig. 3b, high field), the cleavage occurs through the boundaries of alumina cells instead of the pore centers, indicating that the junction strength of the cells is lower than that of the cell walls. The separation of alumina cells was found to be further enhanced with increasing electric field. Figure 4a demonstrates a transverse fracture section near the cutting edge of the PAA film obtained at 70 V. It clearly shows the perfect hexagonal alumina cells with apparent boundaries (see arrows in Fig. 4a), indicating a cell separation caused by a shearing stress during cutting. Figure 4b exhibits alumina nanotubules fabricated from the specimen of Figure 4a by mechanical abrasion and chemical etching. The alumina at the triple junction of three neighboring cells (arrow A in Fig. 4b)

ADVANCED MATERIALS

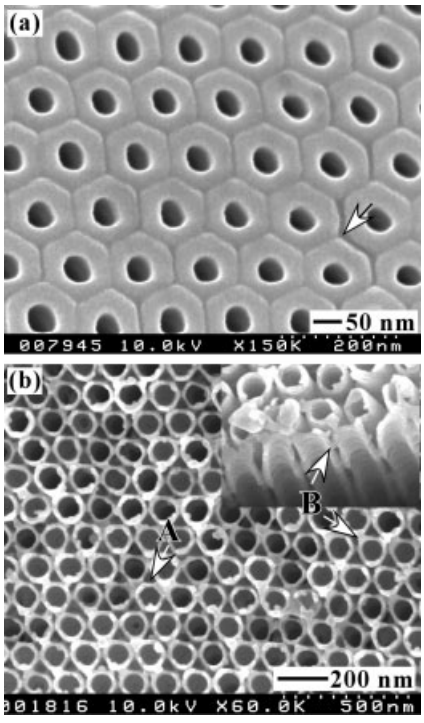

Figure 4. FESEM image of an integrated alumina nanotubule array a) before and b) after chemical etching. The insert in b is a tilted fracture sectional image. (Anodization: 70 V, 2000 A m^{-2}.)

is preferentially removed, while the junction sites between the cells (arrows B in Fig. 4b) remain connected, thus leading to an integrated alumina nanotubule array on aluminum.

The cell separation in PAA films can be ascribed to the interacting repulsive force produced from volume expansion during film growth, which is a characteristic of PAA films formed in sulfuric acid solutions at high potentials.[24–26] The repulsive force increases with film-growth rate, i.e., the high field of high potential and current density, thus leading to a high stress concentrated at the boundaries of alumina cells. The aluminum oxide at the triple cell junction may not be as dense as the other parts of the cell walls, due to the circularly distributed expansion force from the centers of the alumina cells, thus leading to the preferential dissolution of the triple-junction sites. Moreover, Ono et al.[25] and Mei et al.[26] found that the arrayed circular voids were situated vertically at the triple junctions along the alumina cells, and that the size of the voids increases as the applied anodizing potentials increase.[25] The existence of voids at the cell boundaries may reduce the joint strength between cells and lead to cell separation under high electric field. To elucidate the mechanism of cell separation, comprehensive investigations are needed, so it is not elaborated upon here.

In conclusion, we have successfully fabricated highly ordered nanoporous alumina films and integrated alumina nanotubule arrays by a high-field anodization without any assistance. The approach is simple and cost effective, and is able to fabricate large area products for practical devices. In particular, ideally ordered alumina nanostructures, porous films, and tubule arrays, were successfully achieved by anodization at a critical high field (70 V, 2000 A m^{-2}) corresponding to the sulfuric electrolyte system, which is realized by the present study for the first time. Based on an identical principle, our approach may be used in other electrolyte systems to achieve highly ordered alumina nanostructures with a broad cell-size range for various practical applications.

Experimental

Highly pure aluminum sheets (99.99 %, 15 mm × 30 mm × 1.0 mm, Wako Pure Chemical Industry, Ltd) were used as starting specimens. Anodization was performed in a 10 vol.-% sulfuric acid solution at 8–70 V and 0.1–10 °C, with vigorous magnetic stirring. A powerful cooling system (Coolnics Circulator-CTE42A, Yamato) and a large electrolysis cell (1 L) were used to maintain the low temperatures required for the high-field anodization. Anodization was first carried out at constant current densities of 50–2000 A m^{-2} up to designated potentials and then maintained at the potentials for 20–60 min. The duration of the constant current mode lasted from several seconds to nearly ten minutes, depending on the applied initial current densities. To decrease the influence of film thickness, different anodizing times were adopted, with a short period for high potentials and high current density. To achieve high-field (> 40 V, > 1600 A m^{-2}) anodization, the sulfuric solution was pre-anodized with aluminum electrodes for 10–20 A h, which was determined by a series of preliminary experiments. To fabricate alumina nanotube arrays, the PAA films were first abraded with 1 μm alumina sand paper and then immersed in a 5 vol.-% H_3PO_4 solution at 30 °C for 5 min. The morphology of the specimens was investigated by a field-emission scanning electron microscope (FESEM: S-5000, Hitachi) with an energy-dispersive X-ray analyzer (EDX) after consecutive platinum and tungsten evaporations.

Received: February 25, 2005
Final version: May 12, 2005
Published online: July 18, 2005

[1] R. J. Tonucc, B. L. Justus, A. J. Campillo, C. E. Ford, *Science* **1992**, *258*, 783.
[2] T. W. Whitney, J. S. Jiang, P. C. Searson, C. L. Chien, *Science* **1993**, *261*, 1316.
[3] K. Nielsch, F. Müller, A. P. Li, U. Gösele, *Adv. Mater.* **2000**, *12*, 582.
[4] G. L. Che, B. B. Lakshmi, E. R. Fisher, C. R. Martin, *Nature* **1998**, *393*, 346.
[5] S. Z. Chu, S. Inoue, K. Wada, D. Li, H. Haneda, *J. Mater. Chem.* **2003**, *13*, 866.
[6] K. Nishio, H. Masuda, *Electrochem. Solid-State Lett.* **2004**, *7*, H27.
[7] F. Matsumoto, K. Nishio, H. Masuda, *Adv. Mater.* **2004**, *16*, 2105.
[8] J. P. O'Sullivan, G. C. Wood, *Proc. R. Soc. London, Ser. A.* **1970**, *317*, 511.
[9] H. Masuda, K. Fukuda, *Science* **1995**, *268*, 1466.
[10] H. Masuda, H. Yamada, M. Satoh, H. Asoh, M. Nakao, T. Tamamura, *App. Phys. Lett.* **1997**, *71*, 2770.
[11] H. Asoh, K. Nishio, M. Nakao, T. Tamamura, H. Masuda, *J. Electrochem. Soc.* **2001**, *148*, B152.
[12] I. Mikulskas, S. Juodkazis, R. Tomasiunas, J. G. Dumas, *Adv. Mater.* **2001**, *13*, 1574.
[13] H. Masuda, K. Kanezawa, K. Nishio, *Chem. Lett.* **2002**, *12*, 1218.
[14] N. W. Liu, A. Datta, C. Y. Liu, Y. L. Wang, *App. Phys. Lett.* **2003**, *82*, 1281.
[15] H. Masuda, Y. Matsui, M. Yotsuya, F. Matsumoto, K. Nishio, *Chem. Lett.* **2004**, *33*, 584.

[16] H. Masuda, F. Hasegwa, S. Ono, *J. Electrochem. Soc.* **1997**, *144*, L127.
[17] M. T. Wu, I. C. Leu, M. H. Hon, *J. Vac. Sci. Technol. B.* **2002**, *20*, 776.
[18] A. P. Li, F. Muller, A. Birner, K. Nielsch, U. Gösele, *J. App. Phys.* **1998**, *84*, 6023.
[19] S. Shingubara, K. Morimoto, H. Sakaue, T. Takahagi, *Electrochem. Solid-State Lett.* **2004**, *7*, E15.
[20] S. Ono, M. Saito, H. Asoh, *Electrochem. Solid-State Lett.* **2004**, *7*, B21.
[21] S. Ono, M. Saito, M. Ishiguro, H. Asoh, *J. Electrochem. Soc.* **2004**, *151*, B473.
[22] O. Jessensky, F. Müller, U. Gösele, *Appl. Phys. Lett.* **1998**, *72*, 1173.
[23] K. Nielsch, J. Choi, K. Schwirn, R. B. Wehrspohn, U. Gösele, *Nano Lett.* **2002**, *2*, 677.
[24] D. J. Arrowsmith, A. W. Clifford, D. A. Moth, *J. Mater. Sci. Lett.* **1986**, *5*, 921.
[25] S. Ono, H. Ichinose, N. Masuko, *J. Electrochem. Soc.* **1991**, *138*, 3705.
[26] Y. F. Mei, X. L. Wua, X. F. Shaoa, G. S. Huanga, G. G. Siub, *Phys. Lett. A.* **2003**, *309*, 109.

Synthesis and Upconversion Luminescence of Hexagonal-Phase $NaYF_4$:Yb, Er^{3+} Phosphors of Controlled Size and Morphology**

By *Jing-Hui Zeng*, *Ji Su*, *Zhi-Hua Li*, *Ruo-Xue Yan*, and *Ya-Dong Li**

The study of upconversion (UC) phosphors has grown recently owing to their applications in solid-state lasers,[1] optical-fiber-based telecommunications,[2] illumination,[3] flat-panel displays, and biological labeling,[4] and their ability to increase conversion efficiency in photovoltaic cells.[5] As a biological labeling material, UC fluorescent labels show very low background light as a result of their unique fluorescence properties and high detection limits compared with their traditional counterparts, such as the biological labels: rhodamine,[5] fluorescein isothiocyanates (FITC),[6] cyanine dyes (Cy3, Cy5, and Cy7),[7] and metal and semiconductor nanoparticles.[8] Many rare-earth (RE) fluoride-based phosphors present UC abilities from infrared to visible light,[9] and can convert multiple photons of lower energy into one photon of higher energy. Among these materials, hexagonal-phase $NaYF_4$ is reported as one of the most efficient hosts for performing infrared-to-visible photon conversion when activated by Yb, Er^{3+} ion pairs, whose green emission is ten-times stronger and overall (green-plus-red) emissions are 4.4-times greater than those for cubic-phase $NaYF_4$.[10] Its emission is at least two-times greater than that of YF_3:Yb, Er^{3+} at optimum excitation.[11] When doped with Yb, Er^{3+}, the first photon of infrared irradiation (976 nm) elevates an electron to the $^2F_{5/2}$ level of Yb^{3+} and the ion may decay radiatively from this excited state back to the ground state, or it can transfer the energy to the Er^{3+} ion. This energy transfer can promote an electron from the $^4I_{15/2}$ to the $^4I_{11/2}$ state and from the $^4I_{11/2}$ to the $^4F_{7/2}$ state by an energy-transfer upconversion (ETU) process if the $^4I_{11/2}$ state is already populated. The electron in the Er^{3+} $^4F_{7/2}$ state decays non-radiatively to a slightly lower energy state $^4S_{3/2}$ via a multiphonon relaxation process and green light is emitted by an electron transmission from the $^4S_{3/2}$ state to the ground state (Scheme 1). Usually, to ensure a good population of the Er^{3+} $^4I_{11/2}$ state, eighteen times as many Yb^{3+} ions are added to the lattice in comparison to Er^{3+} ions when using infrared excitation.[12]

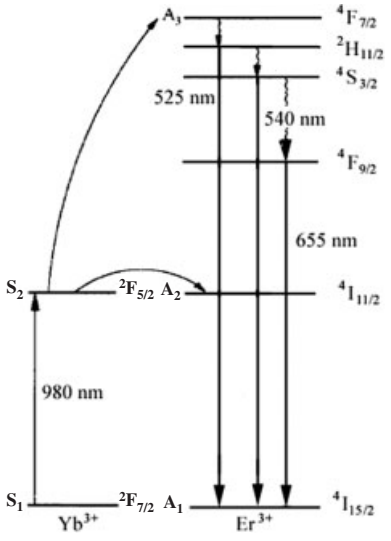

Scheme 1. Scheme of UC spectra of Er^{3+} using Yb^{3+} as the promoter.

The $NaYF_4$:Yb, Er^{3+} UC phosphor was first reported in 1972 by Menyuk et al. who treat YF_3, YbF_3, and ErF_3 in HF gas at 750 °C before a 20 wt.-% excess dried NaF treatment for 16 h at 200 °C and finally at 1000 °C.[11] Kano et al. reported another pathway to the hexagonal $NaYF_4$:Yb, Er^{3+} phosphor.[12] Micrometer-sized $NaYF_4$:Yb, Pr^{3+} was synthesized by Martin et al., whose method included the precipitation of cubic-phase $NaYF_4$ and sand-bath treatment of the product. When the treatment time was extended to ten days, the complete transformation from the cubic phase of $NaYF_4$ to the

[*] Prof. Y.-D. Li, Dr. J.-H. Zeng, J. Su, Dr. Z.-H. Li, R.-X. Yan
Department of Chemistry, Tsinghua University
Beijing, 100084 (P.R. China)
E-mail: ydli@tsinghua.edu.cn
Prof. Y.-D. Li
National Center for Nanoscience and Nanotechnology
Beijing, 100084 (P.R. China)

[**] This work was supported by NSFC (50372030, 20025102, 20131030), the Specialized Research Fund for the Doctoral Program of Higher Education, the Foundation for the Author of National Excellent Doctoral Dissertation of P.R. China, and the State Key Project of Fundamental Research for Nanomaterials and Nanostructures (2003CB716901).

 DOI: 10.1002/adma.200402046